



HAL
open science

Numerical advances in kernels for FDTD Maxwell codes using the Yee algorithm

Filipe José Fernandes Manuel da Silva, Stéphane Heuraux, Bruno Després,
Martin Campos Pinto

► **To cite this version:**

Filipe José Fernandes Manuel da Silva, Stéphane Heuraux, Bruno Després, Martin Campos Pinto. Numerical advances in kernels for FDTD Maxwell codes using the Yee algorithm. 11th International Reflectometry Workshop, Laboratoire de Physique des Plasma-Ecole Polytechnique, Apr 2013, Palaiseau (Ecole Polytechnique), France. hal-04743897

HAL Id: hal-04743897

<https://hal.science/hal-04743897v1>

Submitted on 18 Oct 2024

HAL is a multi-disciplinary open access archive for the deposit and dissemination of scientific research documents, whether they are published or not. The documents may come from teaching and research institutions in France or abroad, or from public or private research centers.

L'archive ouverte pluridisciplinaire **HAL**, est destinée au dépôt et à la diffusion de documents scientifiques de niveau recherche, publiés ou non, émanant des établissements d'enseignement et de recherche français ou étrangers, des laboratoires publics ou privés.



Distributed under a Creative Commons Attribution - NonCommercial - NoDerivatives 4.0
International License

Numerical advances in kernels for FDTD Maxwell codes using the Yee algorithm

F. da Silva, [§]S. Heuroux, [†]B. Després and [†]M. Campos Pinto

*Associação EURATOM/IST–Instituto de Plasmas e Fusão Nuclear
Instituto Superior Técnico, 1046-001 Lisboa, Portugal*

*[§]Intitut Jean Lamour, UMR 7198-CNRS-Univ. Lorraine,
BP 70239, 54506 Vandœuvre Cedex, France*

*[†] Laboratory Jacques Louis Lion, University Pierre et Marie Curie,
Boîte courrier 187, 75252 Paris Cedex 05, France*

Abstract

X-mode FDTD codes, in use, suffer from long-run growth and, under relatively high levels of turbulence, are unstable. The state-of-the art kernel in use for reflectometry simulations, the Xu-Yuan kernel (XYK) [1] is not free from these setbacks. An innovative kernel proposed by Després and Campos Pinto (DPK) addressing these issues and build from scratch to be conservative is being implemented in REFMULX (IPFNs X-mode code). The results obtained with DPK show an improved long-run stability, superior to XYK. Some of the ideas developed in DPK, namely the addressing of fields within each position cell, were applied to the XYK resulting in a modified XYK (MXYK) with a much better performance than the original XYK. This new numerical advance enlarges the possibilities of X-mode simulations in the ITER cases. Although the implementation presented in this work is two-dimensional, these are generic three-dimensional kernels by construction, which makes them of the utmost importance to the 3D reflectometry codes in development.

1 Introduction

One of the most used methods for simulation of propagation of electromagnetic waves in plasmas is Finite-Differences Time-Domain (FDTD) most commonly applied to Maxwell's curl equations [1] although its application to the wave equation is also possible [2]. The usual way to treat the problem is to write the curl equations in a vacuum (with ε_0 and μ_0) and condense the *plasma physics* in the density of current \mathbf{J} .

This results in a system coupling Maxwell equations with a linear vectorial differential equation for \mathbf{J}

$$\begin{aligned} -\varepsilon_0 \partial_t \mathbf{E} + \nabla \times \mathbf{H} &= \mathbf{J} \\ \mu_0 \partial_t \mathbf{H} + \nabla \times \mathbf{E} &= 0 \\ \partial_t \mathbf{J} &= \varepsilon_0 \omega_p^2 \mathbf{E} - \nu \mathbf{J} + \omega_c \mathbf{b} \times \mathbf{J}, \end{aligned} \tag{1}$$

where ν is the frequency of collisions, usually taken as null ($\nu = 0$) in reflectometry simulations.

The curl equations are discretized following Yee schema [1] and a time integrator is used to solve \mathbf{J} . The classic discretization in time for this problem is

$$\begin{aligned}
\varepsilon_0 \frac{\mathbf{E}^{n+1} - \mathbf{E}^n}{\Delta t} - \nabla \times \mathbf{H}^{n+1/2} &= -\mathbf{J}^{n+1} \\
\mu_0 \frac{\mathbf{H}^{n+1/2} - \mathbf{H}^{n-1/2}}{\Delta t} + \nabla \times \mathbf{E}^n &= 0 \\
\frac{\mathbf{J}^{n+1/2} - \mathbf{J}^{n-1/2}}{\Delta t} &= \varepsilon_0 \omega_p^2 \mathbf{E}^n + \omega_c \mathbf{b} \times \frac{\mathbf{J}^{n+1/2} + \mathbf{J}^{n-1/2}}{2}.
\end{aligned} \tag{2}$$

Solving \mathbf{J} for the O-mode, is not problematic and a simple FD integrator can deal with the problem. Solving \mathbf{J} becomes much more delicate when the external magnetic field B_0 plays a role since the term $\omega_c \mathbf{b} \times \mathbf{J}$ couples the different components of \mathbf{E}_\perp and \mathbf{J}_\perp together. Furthermore these crossed components are not usually defined in the same grid points due to the discretization methods used, which adds a complicating factor. Finding a solver which is both stable and efficient must become the challenge. One of the traditionally used techniques was Runge-Kutta of 4th order (RK45) [3]. A numerical scheme proposed by Xu and Yuan, in the context of simulation of Radar Cross Section (RCS) of conduction targets coated by anisotropic magnetized plasmas [4], is being adopted by the simulation reflectometry community and can be considered, up to now, the state-of-art due to its improved stability over the previous ones and also to its computational efficiency. Its first use in reflectometry simulations was in REFMULX code (X-mode), probing a plasma with FMCW (swept reflectometry) using the output data given by the gyrofluid code GEMR as input parameters [6].

2 The Xu-Yuan Kernel (XYK)

The numerical scheme proposed by Xu and Yuan in [4] takes the classic general formulation presented in Eqs. (1). To solve for \mathbf{J} , the inverse Fourier transforms of the Fourier representations of the vectorial components of the LDE are taken and discretized using Yee's notation. Using a central approximation to this integration expansion a discrete representation of $\mathbf{J}_{x,y,z}$ is obtained, where the components of the density current appear time coupled in a system that must be solved simultaneously. Solving it conducts to the explicit discrete expressions for \mathbf{J}_x , \mathbf{J}_y and \mathbf{J}_z .

These, in the 2D implementation of XYK used in REFMULX, without collisions ($\nu = 0$), reduces to

$$\begin{aligned}
J_x^{n+1/2} &= \frac{1 - \frac{\omega_c^2 \Delta t^2}{4}}{1 + \frac{\omega_c^2 \Delta t^2}{4}} J_x^{n-1/2} - \frac{\omega_c \Delta t}{1 + \frac{\omega_c^2 \Delta t^2}{4}} J_y^{n-1/2} + \frac{\varepsilon_0 \omega_p^2 \Delta t}{1 + \frac{\omega_c^2 \Delta t^2}{4}} \left(E_x^n - \frac{\omega_c \Delta t}{2} E_y^n \right) \\
J_y^{n+1/2} &= \frac{1 - \frac{\omega_c^2 \Delta t^2}{4}}{1 + \frac{\omega_c^2 \Delta t^2}{4}} J_y^{n-1/2} + \frac{\omega_c \Delta t}{1 + \frac{\omega_c^2 \Delta t^2}{4}} J_x^{n-1/2} + \frac{\varepsilon_0 \omega_p^2 \Delta t}{1 + \frac{\omega_c^2 \Delta t^2}{4}} \left(E_y^n + \frac{\omega_c \Delta t}{2} E_x^n \right).
\end{aligned} \tag{3}$$

Plasma density $n_e(r, t)$ is introduced in the definition of $\omega_p^2 = n_e e^2 / \varepsilon_0 m_e$ and the external magnetic field $B_0(r, t)$ through $\omega_c = e B_0 / m_e$.

As referenced before and observed in Eqs. (3), the equations are coupled in space. In order to calculating J_x , the knowledge of J_y and E_y , which are not defined in the same grid points as J_x (and E_x), is needed (see Fig. 1—left). The complementary situation exists at the moment of calculating J_y . J_x and E_x are not known at the J_y location (Fig. 1—right). To refer all fields to the same grid point, Xu and Yuan preconize in their paper the use of averages [4]. Implementing that, conducts to an average of J_y and E_y on the 4 points nearest to the one where J_x is being calculated (see Fig. 1—left). For instance, the averaged \hat{J}_y is obtained as

$$\hat{J}_y^{n-1/2}(i, j + 1/2) = \frac{1}{4} \sum_{\substack{i=i \pm 1/2 \\ j=j, j+1}} J_y^{n-1/2}(i, j) \tag{4}$$

and the averaged \widehat{E}_y

$$\widehat{E}_y^{n-1/2}(i, j + 1/2) = \frac{1}{4} \sum_{\substack{i=i\pm 1/2 \\ j=j, j+1}} E_y^{n-1/2}(i, j). \quad (5)$$

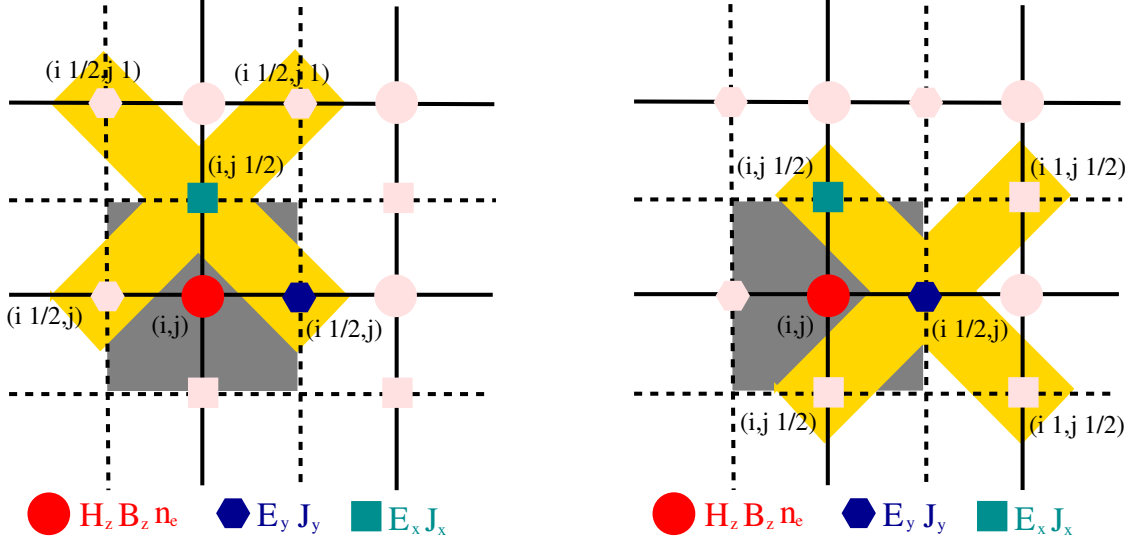


Figure 1: On the left the average stencil used in XYK to calculate \widehat{J}_y and \widehat{E}_y averages and on the right the stencil for the evaluation of \widehat{J}_x and \widehat{E}_x averages.

In the same manner, the average fields \widehat{J}_x and \widehat{E}_x are used in the evaluation of J_y (see Fig. 1—right).

3 Implementation of the Després-Pinto Kernel

The general equations for the new schema proposed by Després-Pinto change the time centering of \mathbf{J} which corresponds to relate \mathbf{J} and \mathbf{E} in a Crank-Nicolson way.

$$\begin{aligned} \varepsilon_0 \frac{\mathbf{E}^{n+1} - \mathbf{E}^n}{\Delta t} - \mathbf{R}\mathbf{H}^{n+1/2} &= -\frac{\mathbf{J}^{n+1} + \mathbf{J}^n}{2} \\ \mu_0 \frac{\mathbf{H}^{n+1/2} - \mathbf{H}^{n-1/2}}{\Delta t} &= -\mathbf{R}^T \mathbf{E}^n \\ \frac{\mathbf{J}^{n+1} - \mathbf{J}^n}{\Delta t} &= \varepsilon_0 S^n(\omega_p^2) \frac{\mathbf{E}^n + \mathbf{E}^{n+1}}{2} + S^n(\omega_c) \mathbf{b} \wedge_h^n \frac{\mathbf{J}^{n+1} + \mathbf{J}^n}{2}, \end{aligned} \quad (6)$$

the operators \mathbf{R} and \mathbf{R}^T implement $\nabla \times \mathbf{H}$ and $\nabla \times \mathbf{E}$ on a Yee cell. $S(u)$ is an operator that implements the multiplication of a vectorial field by a scalar u and $\mathbf{b} \wedge_h$ an operator that approximates the cross product of $\mathbf{b} \times$ on staggered grids.

In the 2D implementation of the DPK in REFMULX, having as a reference the Yee cell shown in Fig. 2, the currents $J_{x,y}$ are obtained as

$$\begin{aligned} J_x^{n+1/2}(i, j + 1/2) &= \frac{1}{1 + \gamma^2} [C_x(i, j) - \gamma C_y(i, j)] \\ J_y^{n+1/2}(i + 1/2, j) &= \frac{1}{1 + \gamma^2} [C_y(i, j) + \gamma C_x(i, j)], \end{aligned} \quad (7)$$

considering

$$\begin{aligned}
C_x(i, j) &= B_x(i, j)/\alpha + \delta/\alpha A_x(i, j) \\
C_y(i, j) &= B_y(i, j)/\alpha + \delta/\alpha A_y(i, j) \\
B_x(i, j) &= J_x^{n-1/2}(i, j + 1/2) + \delta E_x^{n-1/2}(i, j + 1/2) - \beta J_y^{n-1/2}(i + 1/2, j) \\
B_y(i, j) &= J_y^{n-1/2}(i + 1/2, j) + \delta E_y^{n-1/2}(i + 1/2, j) + \beta J_x^{n-1/2}(i, j + 1/2) \\
A_x(i, j) &= E_x^{n-1/2}(i, j + 1/2) + \frac{\Delta t}{\varepsilon_0} (MH)_x(i, j) - \frac{\Delta t}{2\varepsilon_0} J_x^{n-1/2}(i, j + 1/2) \\
A_y(i, j) &= E_y^{n-1/2}(i + 1/2, j) - \frac{\Delta t}{\varepsilon_0} (MH)_y(i, j) - \frac{\Delta t}{2\varepsilon_0} J_y^{n-1/2}(i + 1/2, j) \\
(MH)_x(i, j) &= [H_{zx}^n(i, j + 1) - H_{zx}^n(i, j) + H_{zy}^n(i, j + 1) - H_{zy}^n(i, j)]/\Delta y \\
(MH)_y(i, j) &= [H_{zx}^n(i + 1, j) - H_{zx}^n(i, j) + H_{zy}^n(i + 1, j) - H_{zy}^n(i, j)]/\Delta x,
\end{aligned}$$

with the ancillary constants $\alpha = 1 + \Delta t^2 \omega_p^2/4$, $\beta = 1 + \Delta t \omega_c/2$, $\gamma = \beta/\alpha$ and $\delta = \frac{\Delta t \varepsilon_0 \omega_p^2}{2}$.

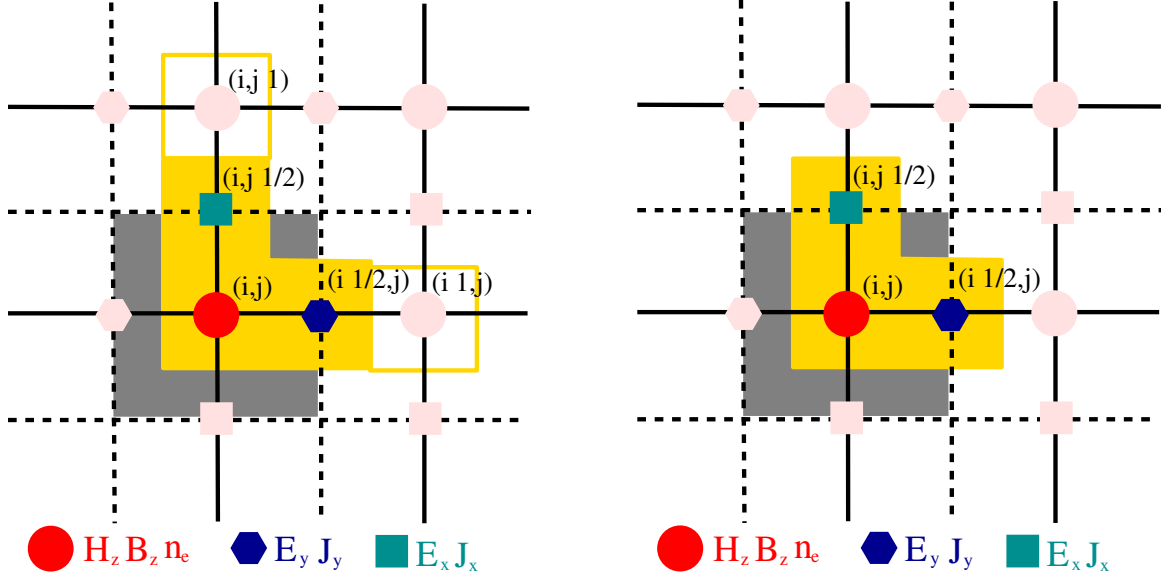


Figure 2: On the right the addressing schema proposed by Després and Campos Pinto. A similar solution is adopted for the XYK, modifying it (MXYK).

As seen in the general Eqs. (6) and its implementation in Eqs. (7), the use of averages as proposed in Xu and Yuan [4], is avoided. In fact, as suggested by Fig. 2, calculations are centered *around an Yee cell*. The equations to update fields H_z and $E_{x,y}$ are discretized following the classic Yee schema.

4 Modified Xu-Yuan Kernel (MXYK)

One of the significant differences between the XYK and the DPK is the use of the averaging schema in XYK. This averaging is not intrinsic to the development of the Xu-Yuan algorithm making its appearance just due to the fact that E_x and J_x are not defined in the same grid positions as E_y and J_y . If we adopt the procedure proposed by Després-Pinto, of centering the calculation on a Yee cell, removing the averages, a modified Xu-Yuan kernel (MXYK) is obtained with improved stability surpassing that of the BDK. This reinforces the idea that the use of averages is a potential source of instability.

5 Simulation tests

The simulations presented in this work to exemplify the behaviour of the different kernels with several levels of turbulence were done on a grid of 1500×1000 grid points ($65.6 \lambda_{35\text{GHz}} \times 43.8 \lambda_{35\text{GHz}}$), using a probing frequency of $f = 35$ GHz. The plasma density $n_e(x)$ is linear, with its edge at $x = 500$ grid points ($21.9 \lambda_{35\text{GHz}}$) and a density gradient length $L_c = 500$ grid points ($21.9 \lambda_{35\text{GHz}}$), for $B_0 = 0$. The turbulence $\delta n_e(x, y)$ has a spectrum with a flat top up to $k = 400 \text{ rad} \cdot \text{m}^{-1}$ from where it decays with a k^{-3} rule [7], [8]. The external magnetic field used in this set of runs was $B_0 = 0.95 \text{ T}$ and the wave is reflected at the upper cutoff f_U . The access frequencies for the upper cutoff are shown in Fig. 3, left, for the unperturbed case ($\delta n_e = 0\%$) and for three levels of homogeneous RMS turbulence $\delta n_e/n_e = 10\%$, 30% and 50% . The field reflected is picked-up in the waveguide, decoupled from the stronger emission signal, through the use of an UTS [10]. With the XYK these signal are shown in Fig. 3 (right) in a logarithmic scale. We can see that for the lower level of turbulence the simulation signal is *stable* up to $\approx 40 \times 10^3$ iterations and for the highest value, breaks around $\approx 5 \times 10^3$. Simulations shown in [6], using the same kernel in swept reflectometry (FMCW) are stable during 120,000 iterations sweeps but the level of turbulence is much lower which attests for the importance of the turbulence levels in the (un)stability of a code. The levels of turbulence used in this work, with an homogeneous radial profile of $\delta n_e/n_e$, are somewhat higher than the expected in experimental cases. Its use is justified to push the code to an upper limit of *numerical robustness* improving ones confidence in its use. Nevertheless, it should be pointed out that these turbulence values show up, not as homogeneous turbulence but in localized zones of the plasma, as measured experimentally [9] and therefore such high values must be used, with the appropriate radial profile of amplitude fluctuations in order to have realistic simulations. Since, as simulations have shown, instabilities can be triggered locally, this set up is of extreme relevance in what concerns long run realistic simulations. For the matrices used and with this simulation setup, the value of 10% is a border value between stability and instability. For a given realization of the matrix, simulations can finish in a stable manner and for other an instability can be triggered confirming the need to have exhaustive tests when programming a code.

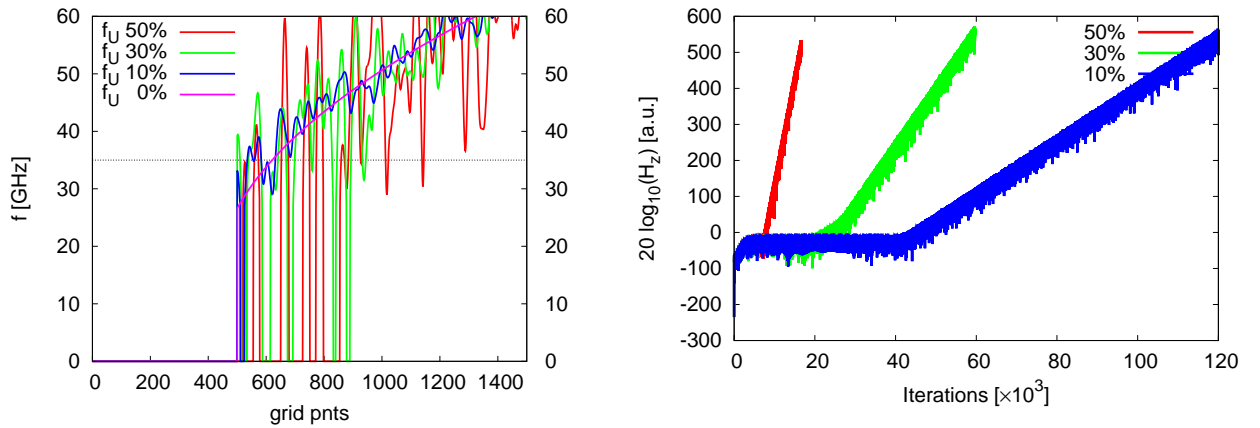


Figure 3: On the left the upper cutoff frequency antenna axial cut for the unperturbed case (0%) and for three levels of RMS turbulence (10%, 30% and 50%). On the right, the plasma return signal for the XYK during a long simulation run, for different levels of turbulence.

Using the MXYK the exact same simulations discussed earlier were performed and the results displayed in Fig. 4 on the right (on the left, are the previous results with the XYK, now in an enlarged scale). The modifications done resulted in a much robust kernel, which for the simulated cases, is stable for 840,000 iterations even for the case of higher turbulence.

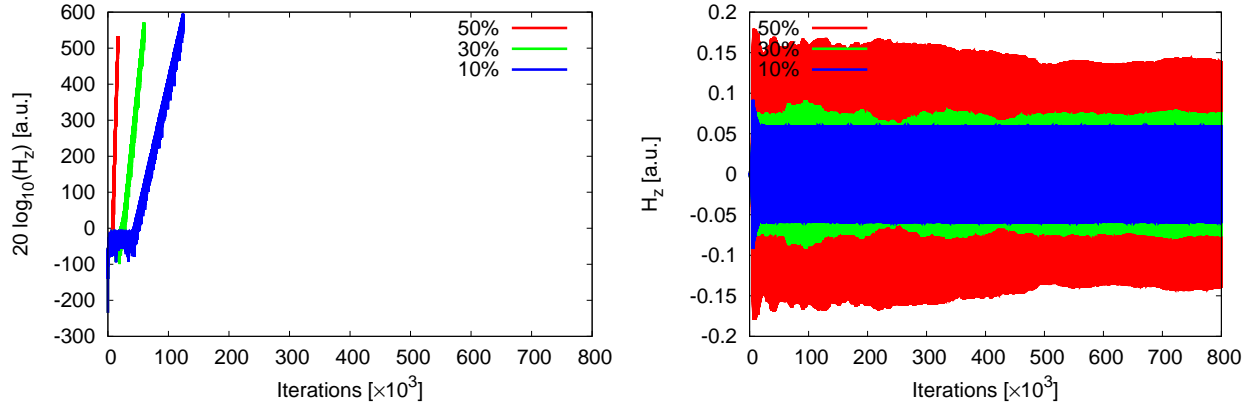


Figure 4: On the left appear long runs (840×10^3 iterations) using the XYK on the left (unstable) and the MXYK on the right (stable) for three levels of turbulence, 10%, 30% and 50%.

6 Conservation of energy

The new kernel proposed is built from the base, assuming conservation of energy and the first tests on the conservative nature of the 2D implementation are on the way, together with the comparison with the behavior of the modified and original Xu-Yuan kernels in what energy conservation is concerned.

7 Conclusions

A new conservative kernel has been proposed by Bruno D espres and Martin Campos Pinto (DPK) and is being implemented in REFMULX code. Using some of the ideas being developed in DPK, concerning the addressing of the discretized quantities on the Yee staggered grids, a modified version of the XYK was obtained (MXYK), without the averaging schema originally proposed by Xu and Yuan. This MXYK offers an enlarged stability during long runs and with very high levels of turbulence and, in all the cases simulated, proved to be stable, unlike the other kernels tested. Longer simulations are now possible with REFMULX, covering a wider range of physics, for instance forward scattering simulations, matching the O-mode fixed frequency performance of REFMUL (O-mode code). More tests are planned using the new kernel(s), namely in FMCW and with dynamic plasma, and in a wider range of plasma scenarios. Another topic that will be pursued is research in the conservative nature of the kernels.

Acknowledgments

This work was supported by EURATOM and carried out within the framework of the European Fusion Development Agreement. IST activities also received financial support from *Funda ao para a Ci encia e Tecnologia* through project Pest-OE/SADG/LA0010/2011. The views and opinions expressed herein do not necessarily reflect those of the European Commission.

IJL activities received support from ANR CHROME (ANR-12-BS01-0006-03).

References

- [1] Kane Yee, Numerical solution of initial boundary value problems involving Maxwell’s equations in isotropic media. IEEE Transactions on Antennas and Propagation **14** (3): 302–307 (1966).

- [2] R. Courant, K. Friedrichs and H. Lewy, Über die partiellen Differenzgleichungen der mathematischen Physik. *Mathematische Annalen* **100(1)**: 32–74 (1928).
- [3] S.D. Conte, C. de Boor, *Elementary Numerical Analysis*, 3rd ed, McGraw-Hill int. ed, (1980).
- [4] Lijun Xu and Naichang Yuan, FDTD Formulations for Scattering from 3-D Anisotropic Plasma Objects, *IEEE Antennas and Wireless Propagation Letters* **5** (2006).
- [5] Bruno Després and Martin Campos Pinto. Notes sur la stabilité du schéma de Yee couplé avec un courant linéaire. *Private notes* (2012).
- [6] F. da Silva, S. Heuraux, T. Ribeiro and B. Scott, Development of a 2D full-wave JE-FDTD Maxwell X-mode code for reflectometry simulation, IRW9, Lisbon, (2009).
- [7] F. da Silva, S. Heuraux, E. Z. Gusakov, and A. Popov, A Numerical Study of Forward- and Backscattering Signatures on Doppler-Reflectometry Signals. *IEEE Transactions On Plasma Science*, **38(9)**: 2144-2149 (2010).
- [8] P. Devynck, X. Garbet, C. Laviron, J. Payan, S. K. Saha, F. Gervais, P. Hennequin, A. Quemeneur, and A. Truc, Localized measurements of turbulence in the TORE SUPRA tokamak, *Plasma Phys. Control. Fusion*, **35 (1)**:63, (1993).
- [9] L. Vermare, S. Heuraux, F. Clairet, G. Leclert, and F. D. Silva, Density fluctuation measurements using X-mode fast sweep reflectometry on Tore Supra. *Nuclear Fusion*, **46(9)**, S743-S759, (2006).
- [10] F. da Silva, S. Heuraux, S. Hacquin, and M. Manso, Unidirectional transparent signal injection in finite-difference time-domain electromagnetic codes—application to reflectometry simulations. *Journal of Computational Physics*, **203(2)**, 467-492, (2005).